Addressing the Challenges of Modeling the Scattering from Bottlebrush Polymers in Solution

Daniel F. Sunday[1], Tyler B. Martin[1], Alice B. Chang[2], Adam B. Burns[1], Robert H. Grubbs[2]

1. Materials Science and Engineering Division, National Institute of Standards and Technology, Gaithersburg, MD 20899, United States
2. Division of Chemistry and Chemical Engineering, California Institute of Technology, Pasadena, CA 91125, United States

Supplemental Information

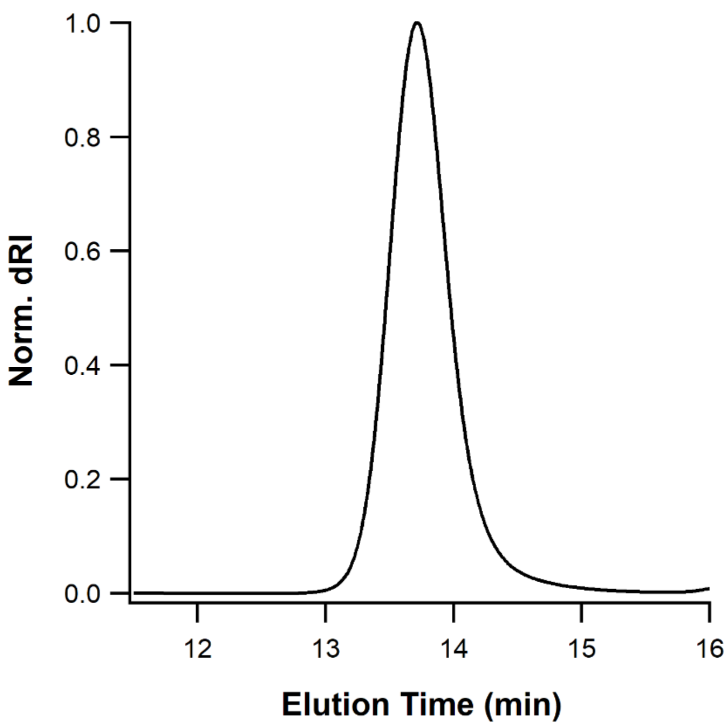

Figure S1: SEC data were collected using two Agilent PLgel MIXED-B 300 × 7.5 mm columns with 10 μm beads. The columns were connected in series with an Agilent 1260 pump, Wyatt 18-angle DAWN HELEOS light scattering detector, and Optilab rEX differential refractive index detector. The mobile phase was THF, and the flow rate was 1 mL/min.

The analysis of PNB_{208}-g_{52}-PS_{40} (N_{BB} = 208, N_{Sc} = 40 at 52 % graft density) in d8-toluene at a volume fraction (ϕ) =0.0014 using both the general Guinier-Porod (GGP) and flexible cylinder models are shown in Figures S2 (scattering pattern and model fit) and S3 (constrained monte-carlo fits for both models). The flexible cylinder model again shows strong correlations between all three structural model parameters (Kuhn length [λ], cylinder length [L_c] and radius [R]) and multiple minima. The GGP model shows negligible correlations although it does exhibit a somewhat shallow minima in the vicinity of the best fit. In spite of this the DREAM algorithm implemented in Sasview reliably found the same minima on multiple runs.

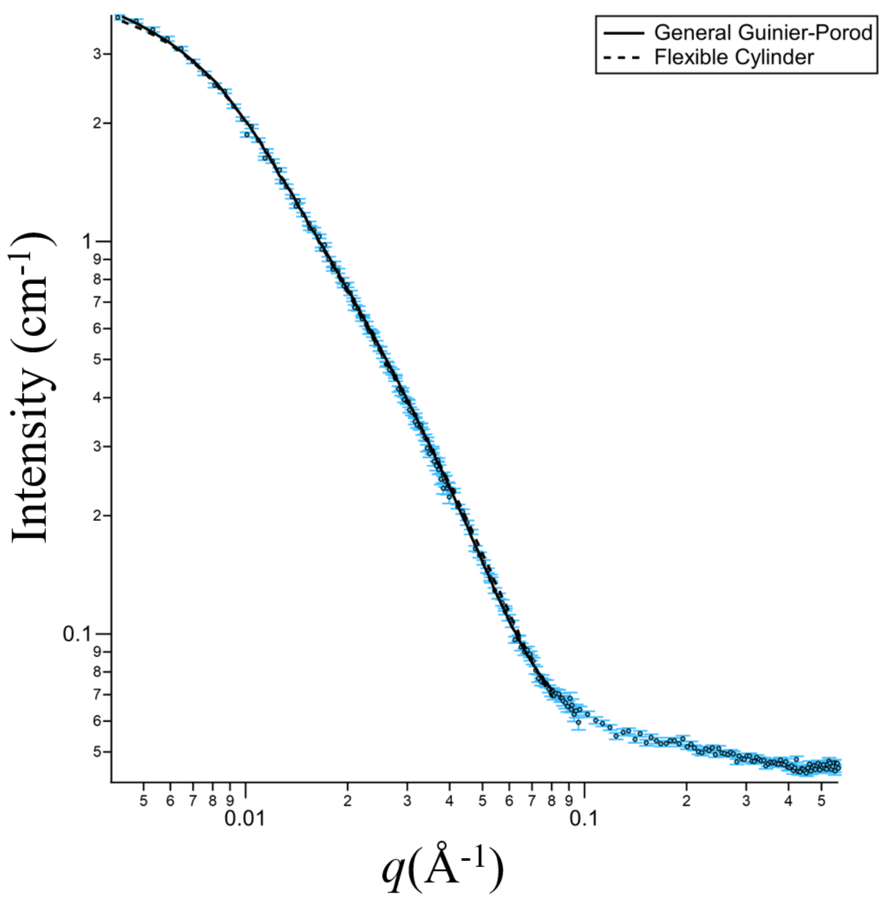

Figure S2: Fits to the scattering data for PNB_{208}-g_{52}-PS_{40} (at a volume fraction of 0.0014 in d8-toluene) with the general Guinier-Porod model and the flexible cylinder model. Both models provide excellent fits to the data. Correlation maps and GF as a function of L_c and $R_{g,2}$ are shown in S3A and S3B, respectively.

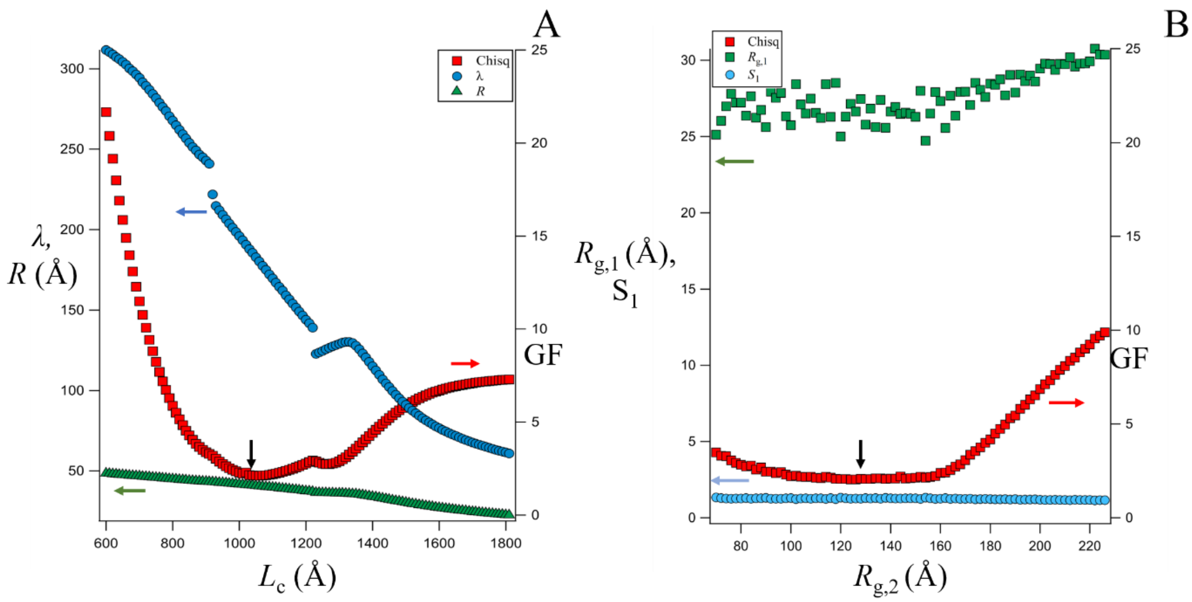

Figure S3: Fits to the scattering data from the PNB_{208}-g_{52}-PS_{40} bottlebrush at a volume fraction of 0.0014 in d8-toluene. A) Results of the parameter mapping performed by holding L_c constant and allowing λ and R to vary during fits with the flexible cylinder model. D) Results of the correlation mapping from the Generalized Guinier-Porod model, holding $R_{g,2}$ constant and allowing the other parameters to vary. Vertical arrows in A and B correspond to the fits shown in S2.

The final sample that was examined consisted of a much longer backbone with slightly longer sidechains at 100 % graft density (PNB_{482}-g_{100}-PS_{62}, N_{BB} = 482, N_{Sc} = 62) in d8-toluene, ϕ = 0.002. Compared to the samples examined previously this is expected to have a greater persistence length and be more highly extended due to the longer backbone and sidechains. Surprisingly, the flexible cylinder model was not able to accurately match the scattering, with the best fit underpredicting the low q scattering (shown in Figure S4). The GGP model was able to accurately recreate the experimental scattering profile, and the ratio of the long and short R_g axis (R_{g1}/R_{g2} = 7.02) show a highly anisotropic shape. Constrained monte-carlo modeling again shows strong correlations between model parameters for the flexible cylinder, which are absent in the GGP.

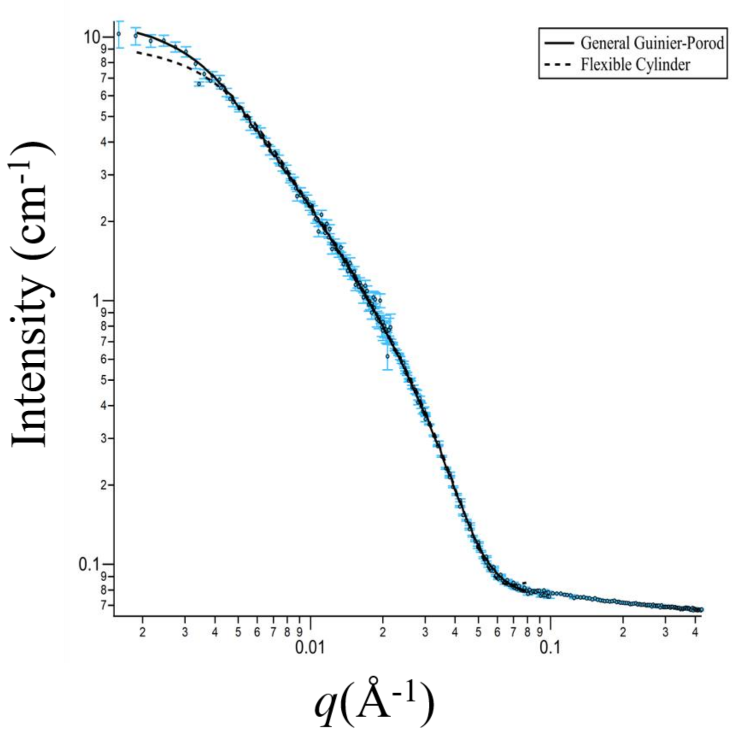

Figure S4: Fits to the scattering data for PNB_{482}-g_{100}-PS_{62} (at a volume fraction of 0.002 in d8-toluene).with the general Guinier-Porod model and the flexible cylinder model. Correlation maps and GF as a function of L_c and $R_{g,2}$ are shown in S5A and S5B, respectively.

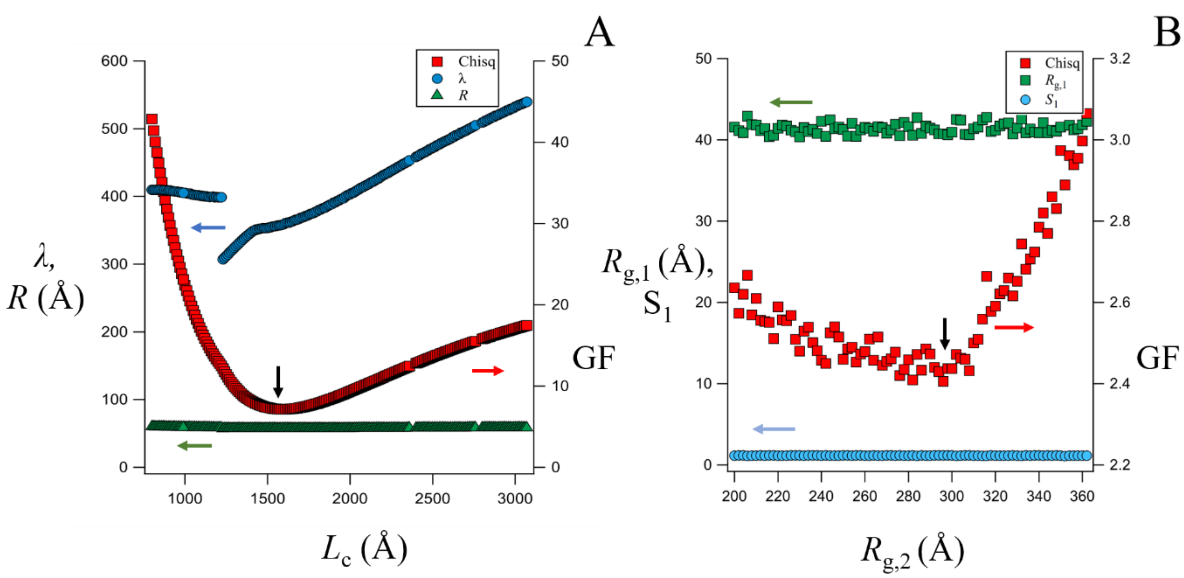

Figure S5: Fits to the scattering data from the PNB_{482}-g_{100}-PS_{62} bottlebrush at a volume fraction of 0.002 in d8-toluene. A) Results of the parameter mapping performed by holding L_c constant and allowing λ and R to vary during fits with the flexible cylinder model. D) Results of the correlation mapping from the

Generalized Guinier-Porod model, holding $R_{g,2}$ constant and allowing the other parameters to vary. Vertical arrows in A and B correspond to the fits shown in S4.

Table S1: Best fits to the three samples using the Generalized Guinier-Porod Model

Sample	Volume Fraction	$R_{g,2}$ (Å)	$R_{g,1}$ (Å)	s_1	l_p (Å)
PNB_{482}-g_{100}-PS_{62}	0.002	285.9±11.2	40.1±0.4	1.19±0.01	89.6±7.3
PNB_{208}-g_{52}-PS_{40}	0.0014	123.1±6.7	23.1±0.8	1.37±0.02	38.5±3.4
PNB105-g_{100}-PS_{40}	0.005	89.0±1.4	25.7±0.4	1.30±0.02	47.8±0.9

Table S2: Literature Data from Figure 2

Abbreviation Guide	
PHEMA	Poly (hydroxy ethyl metharylate)
PNBA	poly (n-butyl acrylate)
PMMA	Poly(Methyl methacrylate)
PS	Polystyrene
PNB	Poly (norbornene)
PLA	Poly(lactic acid)
PEG	Poly(ethylene glycol)
PNHI	poly(n-hexyl isocyanate)
N_{BB}	Backbone Degree of polymerization
N_S	Sidechain degree of polymerization
ϕ	Volume Fraction
R (nm)	Cylinder Radius
L_c (nm)	Cylinder Length
l_p (nm)	Persistence Length

Publication Title	Year	BackBone Classification	Backbone Polymer	Sidechain	Solvent	N_{BB}	N_S	ϕ	R (nm)	L_c (nm)	l_p (nm)
On the Shape of Bottle-Brush Macromolecules: Systematic Variation of Architectural Parameters	2005	Vinyl	PHEMA	PNBA	Toluene	400	22	0.0025	4.2	112	70
	2005	Vinyl	PHEMA	PNBA	Toluene	400	62	0.0025	6.3	113	70
	2005	Vinyl	PHEMA	PNBA	Toluene	400	98	0.0025	8.2	151	70
	2005	Vinyl	PHEMA	PNBA	Toluene	188	58	0.0025	6.0	77	70
	2005	Vinyl	PHEMA	PNBA	Toluene	780	50	0.0025	5.8	223	70
Chain Conformation of Cylindirical Brushes in Solution	2006	Vinyl	PMMA	PS	cyclohexane	9445	7.6	0.001	1.3	1476	4.7
	2006	Vinyl	PMMA	PS	cyclohexane	1816	9.6	0.001	1.4	315	5.3
	2006	Vinyl	PMMA	PS	cyclohexane	2668	13.1	0.001	1.6	494	6.2
	2006	Vinyl	PMMA	PS	cyclohexane	1649	17.1	0.001	1.9	307	8.5
	2006	Vinyl	PMMA	PS	cyclohexane	2145	22.1	0.001	2.2	388	10.8
	2006	Vinyl	PMMA	PS	cyclohexane	1023	34.8	0.001	3.0	189	17.8
	2006	Vinyl	PMMA	PS	Toluene	9445	7.6	0.001	1.3	1618	4.4
	2006	Vinyl	PMMA	PS	Toluene	1816	9.6	0.001	1.5	352	5.9
	2006	Vinyl	PMMA	PS	Toluene	2668	13.1	0.001	1.7	487	7.6
	2006	Vinyl	PMMA	PS	Toluene	1649	17.1	0.001	2.1	314	11.0
	2006	Vinyl	PMMA	PS	Toluene	2145	22.1	0.001	2.4	394	15.7
	2006	Vinyl	PMMA	PS	Toluene	1023	34.8	0.001	3.4	179	32.1

Publication Title	Year	BackBone Classification	Backbone Polymer	Sidechain	Solvent	N_{BB}	N_S	ϕ	R	L_c	l_p
Bottle-brush Macromolecules in solution: Comparison between results obtained from scattering experiments and computer simulations	2006	Vinyl	PHEMA	PNBA	Toluene	486	9	0.0025	2.6	106	27
	2006	Vinyl	PHEMA	PNBA	Toluene	400	22	0.0025	4.2	112	35
	2006	Vinyl	PHEMA	PNBA	Toluene	365	41	0.0025	5.1	113	35
	2006	Vinyl	PHEMA	PNBA	Toluene	400	62	0.0025	6.3	133	35
	2006	Vinyl	PHEMA	PNBA	Toluene	400	98	0.0025	8.2	151	35
	2006	Vinyl	PHEMA	PNBA	Toluene	188	58	0.0025	6.0	77	35
	2006	Vinyl	PHEMA	PNBA	Toluene	780	50	0.0025	5.8	223	35
Interaction of cylindrical polymer brushes in dilute and semi-dilute solution	2009	Vinyl	PHEMA	PTBA	THF	1600	61	0	5.4	384	17.5
	2009	Vinyl	PHEMA	PTBA	THF	1600	61	0.0007	5.4	384	17.5
	2009	Vinyl	PHEMA	PTBA	THF	1600	61	0.002	5.4	384	17.5
	2009	Vinyl	PHEMA	PTBA	THF	1600	61	0.006	5.4	384	13.5
	2009	Vinyl	PHEMA	PTBA	THF	1600	61	0.013	5.4	384	9.5
	2009	Vinyl	PHEMA	PTBA	THF	1600	61	0.038	5.4	384	5

Publication Title	Year	BackBone Classification	Backbone Polymer	Sidechain	Solvent	N_{BB}	N_S	ϕ	R	L_c	l_p
Small Angle Neutron Scattering Analysis of Bottlebrush Polymers Prepared viaGrafting-Through Polymerization	2013	Norbornene	PNB	PS	Toluene	45	14	0.0115	2.7	15.5	3.4
	2013	Norbornene	PNB	PS	Toluene	260	14	0.0115	2.5	45.5	5.7
	2013	Norbornene	PNB	PS	Toluene	11	20	0.0115	2.5	12.4	2.7
	2013	Norbornene	PNB	PS	Toluene	15	20	0.0115	2.3	15.6	2.6
	2013	Norbornene	PNB	PS	Toluene	120	24	0.0115	2.7	14.6	2.9
	2013	Norbornene	PNB	PS	Toluene	150	42	0.0115	3.7	27.5	3.5
	2013	Norbornene	PNB	PS	Toluene	220	54	0.0115	4.3	51.7	6.5
Small Angle Neutron Scattering Analysis of Bottlebrush Backbone and Side Chain flexibilty	2016	Norbornene	PNB	PLA	1,4-dioxane	25	34	0.01	4.1	8.1	7.1
	2016	Norbornene	PNB	PLA	1,4-dioxane	52	34	0.01	4.2	14.9	9.4
	2016	Norbornene	PNB	PLA	1,4-dioxane	87	34	0.01	4.3	22.8	8.0
	2016	Norbornene	PNB	PLA	1,4-dioxane	144	34	0.01	4	32	8.5
	2016	Norbornene	PNB	PLA	1,4-dioxane	173	34	0.01	3.7	38.6	5.3
	2016	Norbornene	PNB	PLA	1,4-dioxane	38	60	0.01	5.1	15	12.9
	2016	Norbornene	PNB	PLA	1,4-dioxane	97	57	0.01	5	45.1	5.6
	2016	Norbornene	PNB	PLA	1,4-dioxane	147	57	0.01	5.1	46.2	5.8
	2016	Norbornene	PNB	PLA	1,4-dioxane	222	57	0.01	5.2	48.2	6.3

Publication Title	Year	BackBone Classification	Backbone Polymer	Sidechain	Solvent	N_{BB}	N_S	ϕ	R	L_c	l_p
Small angle Neutron Scattering Study of Conformation of oligo(ethylene glycol)-Grafted Polystyrene in Dilute Solutions: Effect of the Backbone Length	2008	Vinyl	PS	PEG	D2O	8	4	0.01	1.6	6.5	NA
	2008	Vinyl	PS	PEG	D2O	40	4	0.01	1.5	7.6	NA
	2008	Vinyl	PS	PEG	D2O	57	4	0.01	1.5	8.8	NA
	2008	Vinyl	PS	PEG	D2O	58	4	0.01	1.4	10.6	NA
	2008	Vinyl	PS	PEG	D2O	85	4	0.01	1.3	13.6	NA
	2008	Vinyl	PS	PEG	Toluene	8	4	0.01	1.2	2.3	NA
	2008	Vinyl	PS	PEG	Toluene	40	4	0.01	1.2	6.1	NA
	2008	Vinyl	PS	PEG	Toluene	57	4	0.01	1.2	8.2	NA
	2008	Vinyl	PS	PEG	Toluene	58	4	0.01	1	13.3	4.1
	2008	Vinyl	PS	PEG	Toluene	85	4	0.01	1	23.9	4.1
	2008	Vinyl	PS	PEG	Methanol	8	4	0.01	1	3.1	NA
	2008	Vinyl	PS	PEG	Methanol	40	4	0.01	1.3	6	NA
	2008	Vinyl	PS	PEG	Methanol	57	4	0.01	1.2	7.7	NA
	2008	Vinyl	PS	PEG	Methanol	58	4	0.01	1.2	14	3.6
	2008	Vinyl	PS	PEG	Methanol	85	4	0.01	1.2	22.1	3.6
Structural evolution of Polylaactide Molecular Mottlebrushes: Kinetics Study by Size Exclusion Chromatography, Small angle Neutron Scattering, and Simulations	2014	Norbornene	PNB	PLA	THF	16	20	0.01	2.3	2	1.8
	2014	Norbornene	PNB	PLA	THF	39	20	0.01	2.3	8.5	4.2
	2014	Norbornene	PNB	PLA	THF	73	20	0.01	2.3	16	10.6
	2014	Norbornene	PNB	PLA	THF	108	20	0.01	2.2	36	6.6
	2014	Norbornene	PNB	PLA	THF	195	20	0.01	2.2	52.3	8.2
	2014	Norbornene	PNB	PLA	THF	260	20	0.01	2.2	53.7	8.2
	2014	Norbornene	PNB	PLA	THF	357	20	0.01	2.2	61.7	9.7
	2014	Norbornene	PNB	PLA	THF	429	20	0.01	2.2	51	10.85
	2014	Norbornene	PNB	PLA	THF	466	20	0.01	2.2	50.8	9.65
	2014	Norbornene	PNB	PLA	THF	483	20	0.01	2.2	54.6	9.5

Publication Title	Year	BackBone Classification	Backbone Polymer	Sidechain	Solvent	N_{BB}	N_S	ϕ	R	L_c	l_p
Determination of the chain stiffness parameter of molecular rod brushes consisting of a polymethymethacrylate main chain and poly(n-hexyl isocyanate) side chains	2015	Vinyl	PMMA	PNHI	THF	385	26	?	9.5	106.3	24
	2015	Vinyl	PMMA	PNHI	THF	418	36	?	13.1	116.7	27.5
	2015	Vinyl	PMMA	PNHI	THF	346	40	?	14.5	99.9	29.5
	2015	Vinyl	PMMA	PNHI	THF	486	46	?	16.5	130.0	40
	2015	Vinyl	PMMA	PNHI	THF	543	58	?	20.8	148.0	48.5
	2015	Vinyl	PMMA	PNHI	THF	844	69	?	24.7	227.4	65
	2015	Vinyl	PMMA	PNHI	THF	356	82	?	29.1	114.9	135
Conformational Properties of Cylindrical Rod Brushes Consisting of a Polystyrene main chain and poly(n-hexyl isocyanate) side chains	2008	Vinyl	PS	PNHI	THF	1070	1	?	0.6	270.0	2.5
	2008	Vinyl	PS	PNHI	THF	270	21	?	2.3	64.6	12.5
	2008	Vinyl	PS	PNHI	THF	308	29	?	2.8	17.8	13.5
	2008	Vinyl	PS	PNHI	THF	201	32	?	3.3	16.1	19
	2008	Vinyl	PS	PNHI	THF	227	62	?	5.8	49.8	29.5
	2008	Vinyl	PS	PNHI	THF	145	80	?	7.1	60.3	38.5

General Guinier-Porod Model

The implementation of the general Guinier-Porod model in Sasview is available in the Sasview marketplace (http://marketplace.sasview.org/), with the model name "2 Layer General Guinier Porod"